Supporting Information for

Liquid acid-catalysed Fabrication of nanoporous 1,3,5-triazine frameworks with efficient and selective CO2 uptake

Shaohui Xiong‡[a], Xian Fu‡[a], Lu Xiang[a], Guipeng Yu[a,*], Jianguo Guan[b], Zhonggang Wang[c,*], Yong Du[d], Xiang Xiong[d] and Chunyue Pan [a,*]

Table of Content

1. Characterization of model compound MC-1

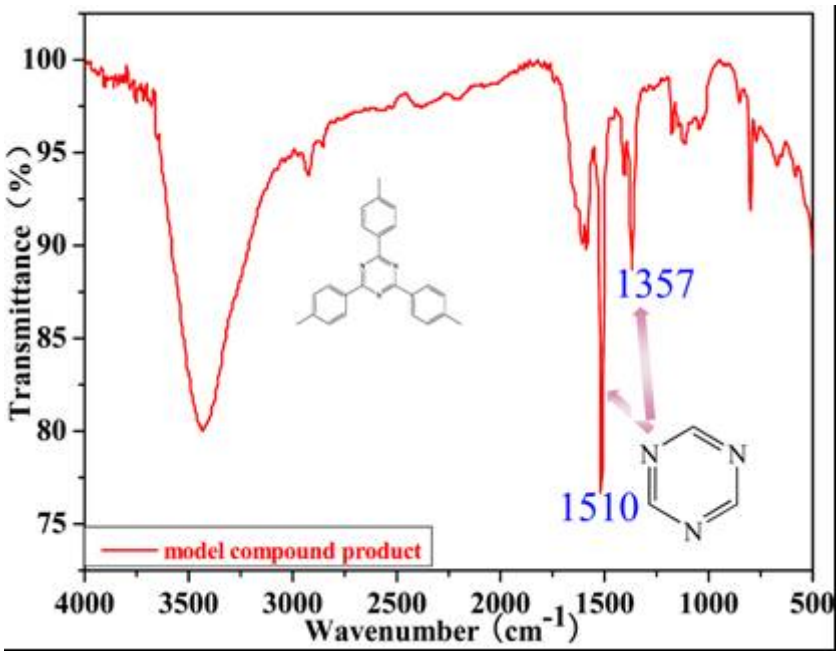

Fig. S1. FT-IR spectrum of model compound MC-1.

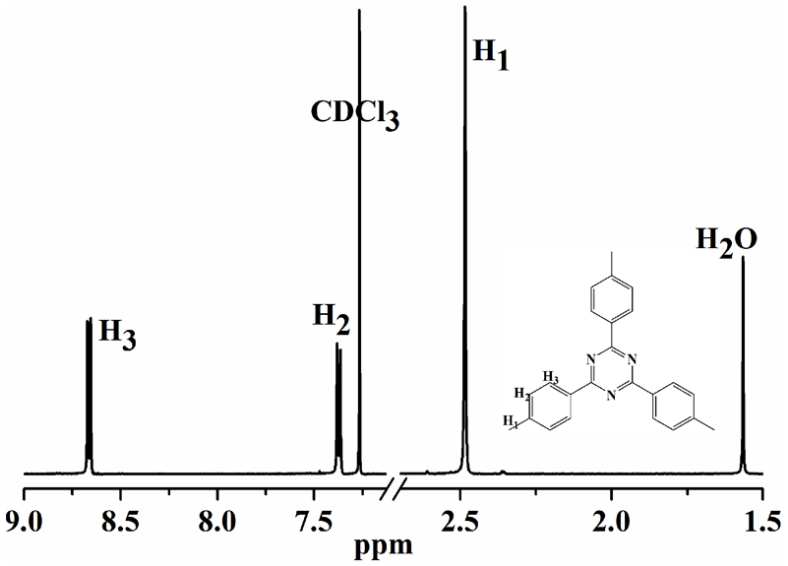

Fig. S2. ^{1}H NMR spectrum of model compound MC-1.

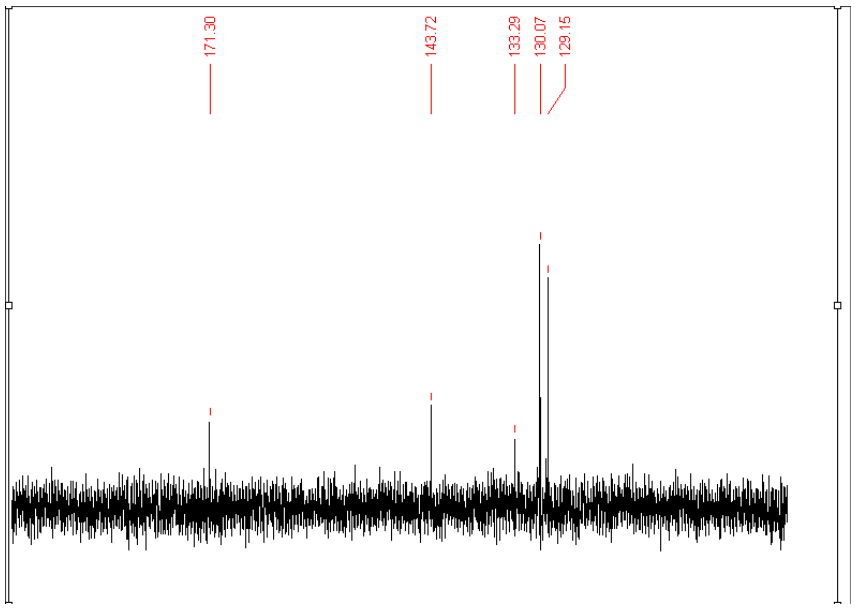

Fig. S3. ^{13}C NMR spectrum of model compound II

2. Synthesis and characterization of model compound MC-2

In a 100 mL round-bottom flask, triphenylamine (2.0 mmol) was charged and then a solution of benzoyl choloride (6.6 mmol) in 50mL o-dichlorobenzene was charged. The solution mixture was stirred for 0.5h and then 2.7 mL (35 mmol) methanesulfonic acid in 200 mL dry o-dichlorobenzene was added dropwisely. The solution mixture was stirred and heated to 140 °C for another 24 hours. Finally, 500 mL of water was added. The crude product was collected by extraction in chloform (3X). The product was purified by column chromatography (CH_2Cl_2/petrol ether V/V=1:1), afford the model compound as a light yellow solid (yield: 87%). ^1H NMR (400 MHz, $CDCl_3$): δ= 7.85-7.82 (m, 4H, Ar-H), 7.60-7.65 (m, 1H, Ar-H), 7.45-7.56 (m, 2H, Ar-H), 7.19-7.30 (m, 2H, Ar-H); ^{13}C NMR (100 MHz, $CDCl_3$): δ= 194.30, 159.13, 148.42, 148.12, 141.23, 140.19, 134.76,131.65, 128.44; IR (KBr, cm^{-1}): 1669 (s), 1601(s), 1588 (w), 1491 (vs), 1412 (m), 1347 (s), 1249 (s), 1016 (m), 801 (m), 796 (vs). TOF/MS. GC/MS (M+ Calcd. as $C_{39}H_{27}NO_3$, 557.1991) m/z: 557.1977 (M+). Calcd. C 84.00, H 4.88, N 2.51; Found. C 83.91, H 4.78, N 2.42.

The reaction of triphenylamine (2.0 mmol) with chlorobenzene was conducted in the same procedure as for the synthesis of MC-2. However, No product was found as detected by TLC and HPLC except the origin starting compounds, even the reaction temperature was raised to 180°C for 48 hours.

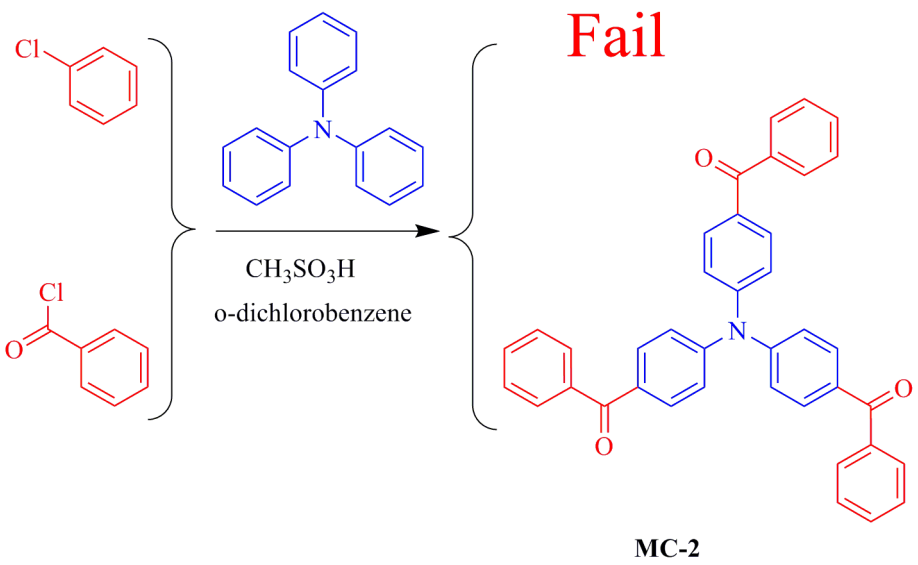

MC-2

Scheme S1. Synthesis of model compound II

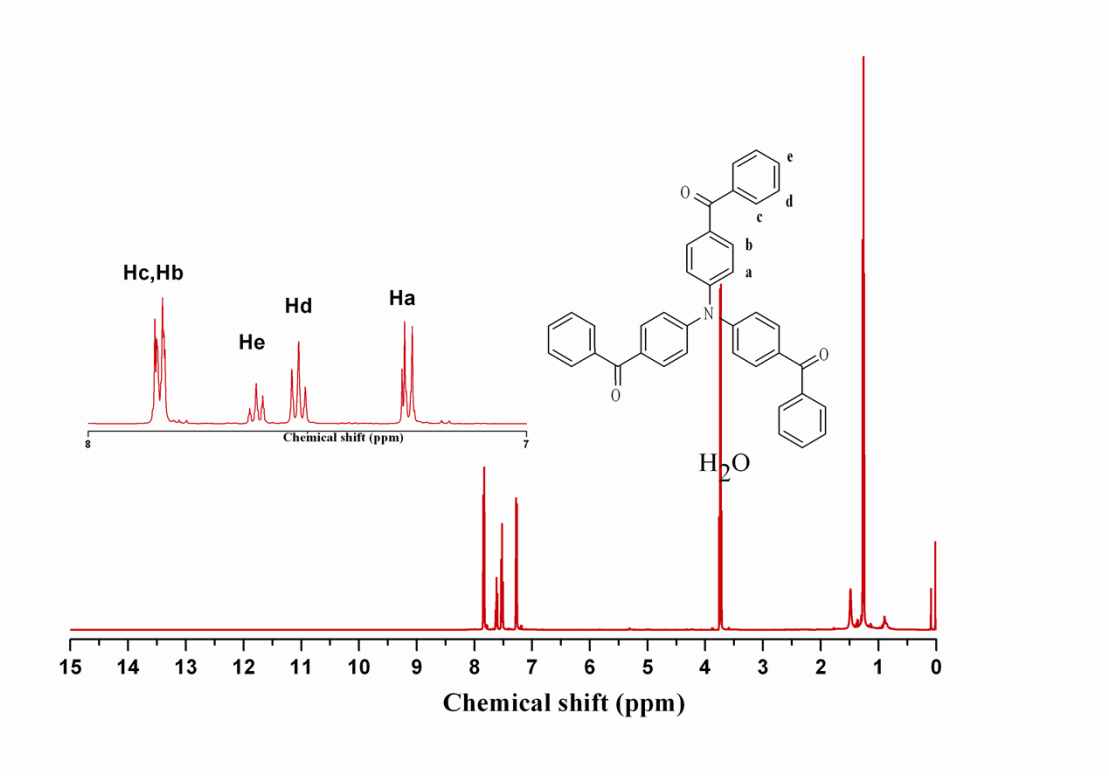

Fig. S4. ^{1}H NMR spectrum of model compound II

3. Synthesis of NOP-7 and NOP-8

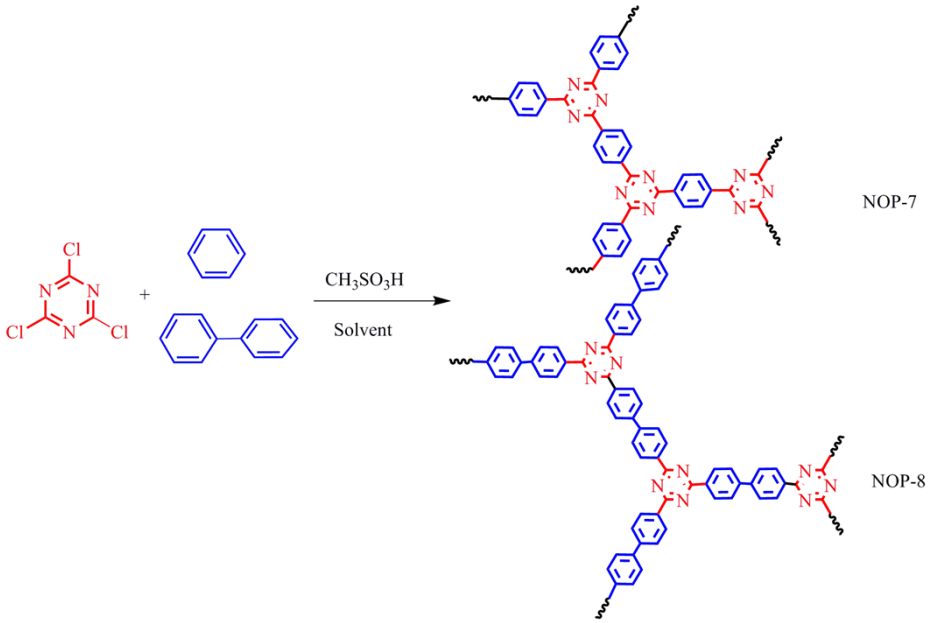

Scheme S2. Synthetic routes of NOP-7 and NOP-8

NOP-7: A mixture of cyanuric chloride (CC, 2 mmol) and benzene (3 mmol) was dissolved in 50 mL of anhydrous and then 2.7 mL (35 mmol) methanesulfonic acid in 200 mL dry o-dichlorobenzene was added dropwisely. The solution mixture was stirred at 140 °C for 24 hours, and then 100 mL of water was added. The crude product was collected by precipitation in water. The precipitate filtered off from the hot reaction mixture was soxhlet extracted over night with methanol, tetrahydrofuran and acetone and dried in vacuum (yield: 5%). Calcd. C 82.33, H 3.95, N 13.72; Found. C 80.89, H 3.65, N 13.38.

NOP-8: The synthesis of NOP-8 was conducted in a similar procedure as for NOP-7 except biphenyl was applied as starting material. The crude product was collected by precipitation in water. The product was obtained as a yellow solid (yield: 11%). Calcd. C 87.62, H 4.52, N 7.86; Found. C 87.03, H 4.38, N 7.69.

4. Adsorption–desorption isotherms and spectras of NOPs(Fig. S5 ~ Fig. S7)

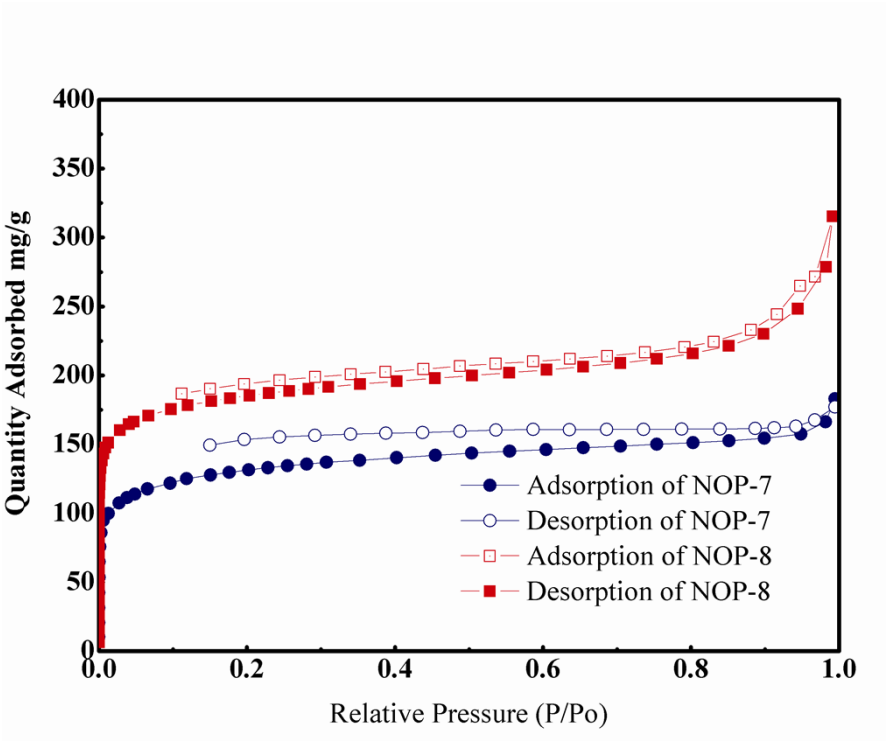

Fig. S5 Nitrogen adsorption–desorption isotherms at 77 K for the polymers.

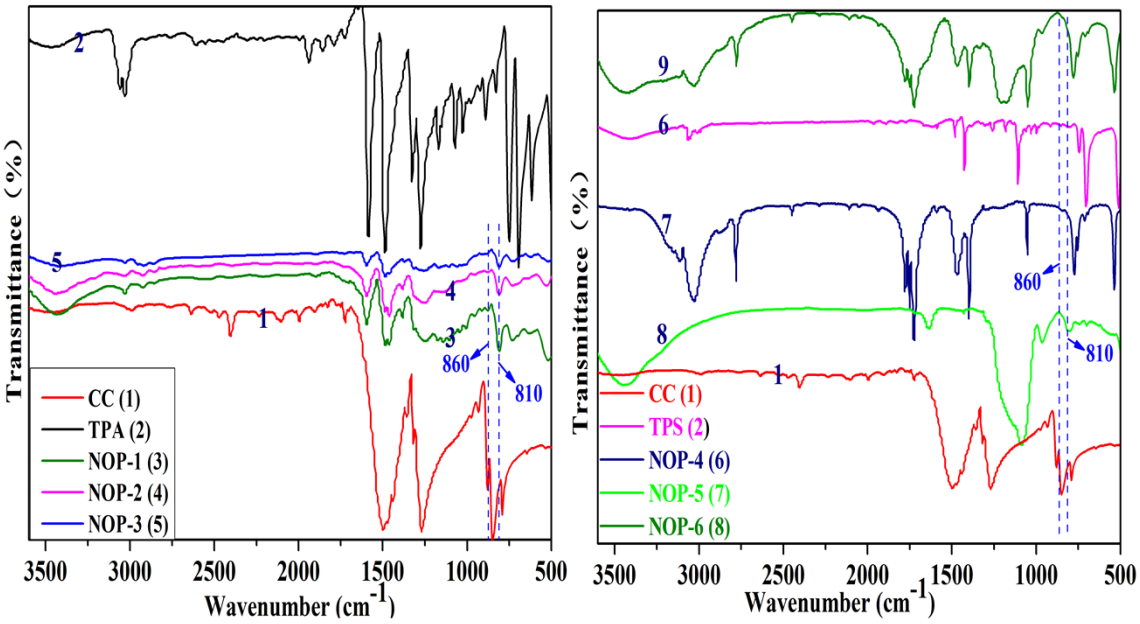

Fig. S6 FT-IR spectra of CC, TPA, TPS and NOP-1~6

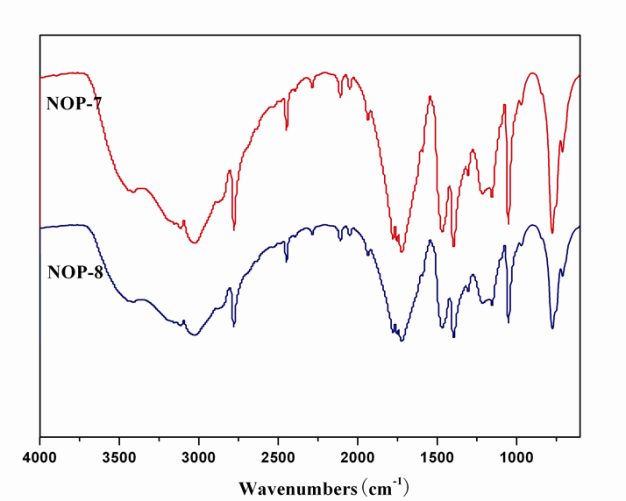

Fig. S6 FT-IR spectra of NOP7 and NOP-8

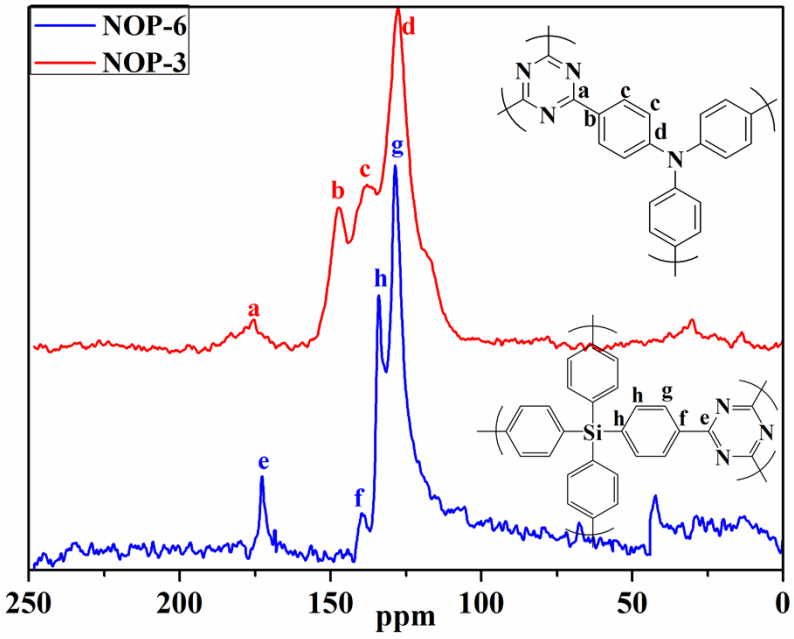

Fig. S7 ^{13}C CP/MAS NMR spectra of NOP-3 and NOP-6

5. UV-Vis and Luminescent spectras of NOP-3 and NOP-6(Fig. S8 and Fig. S9)

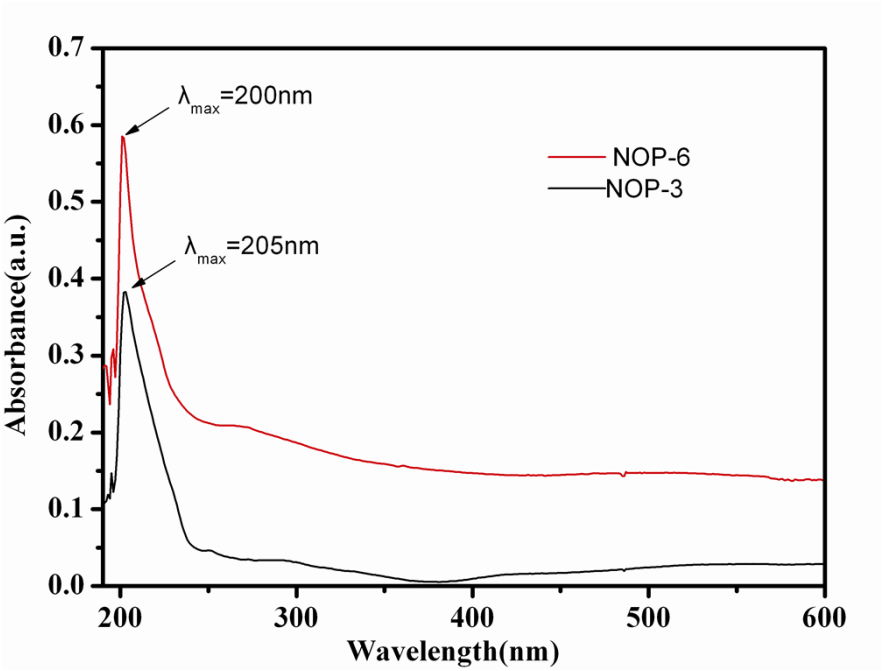

Fig. S8 UV-Vis spectra of NOP-3 and NOP-6 in alcohol

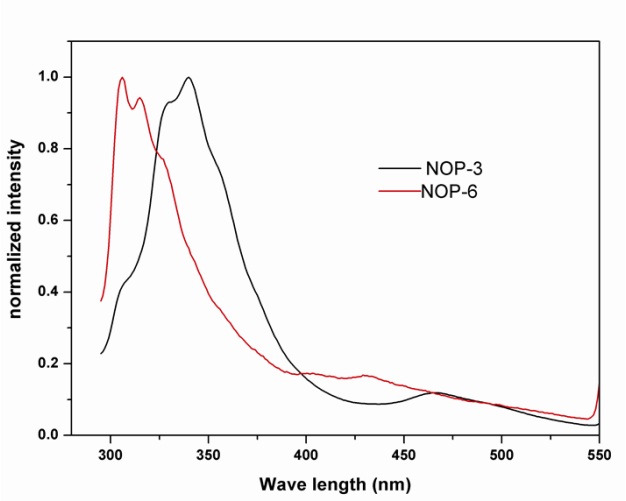

Fig. S9 Luminescent spectra NOP-3 and NOP-6 in alcohol

6. X-ray powder diffraction patterns of NOP-3 and NOP-6(Fig. S10)

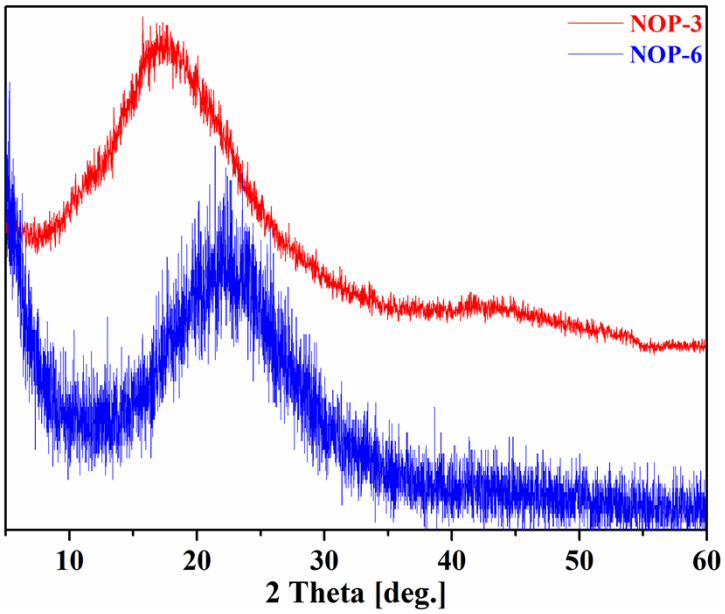

Fig. S10 X-ray powder diffraction patterns of NOP-3 and NOP-6.

7. SEM images for NOP-3 and NOP-6(Fig. S11 and Fig. S12)

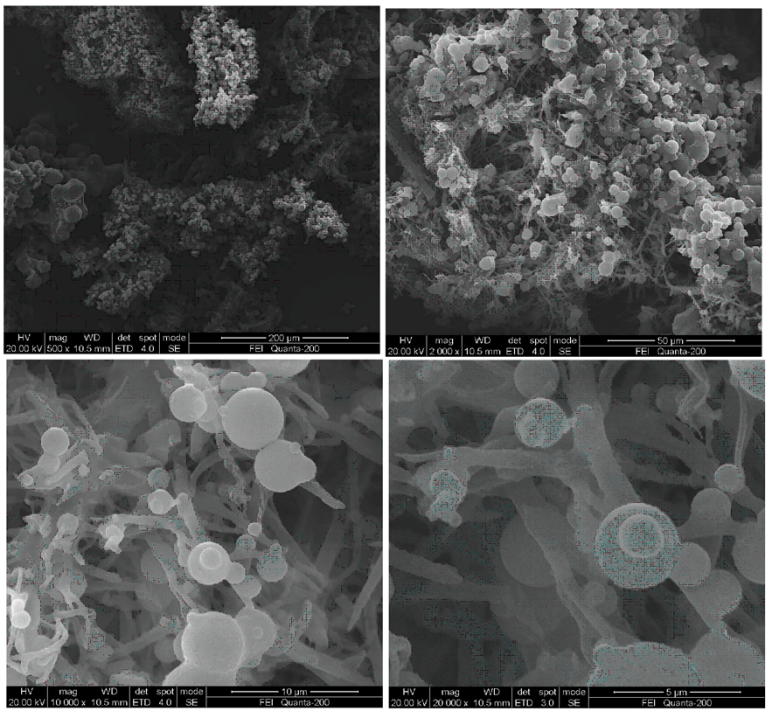

Fig. S11 SEM images for NOP-3.

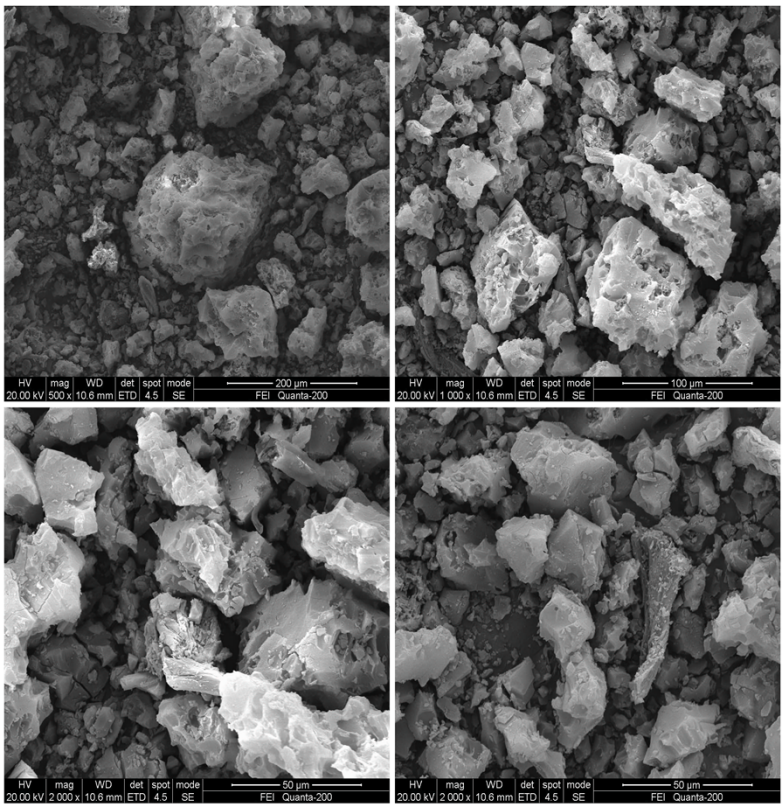

Fig. S12 SEM images for NOP-6.

8. TEM images for NOP-3 and NOP-6(Fig. S13 and Fig. S14)

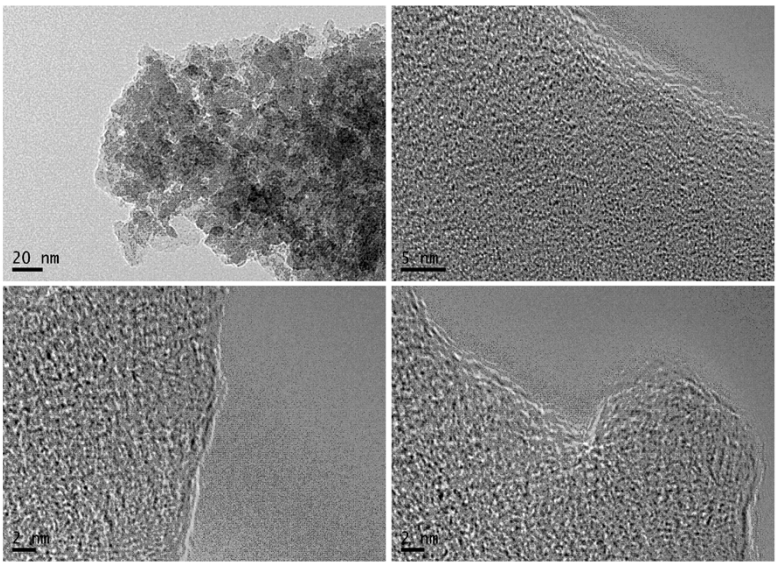

Fig. S13 TEM images for NOP-3.

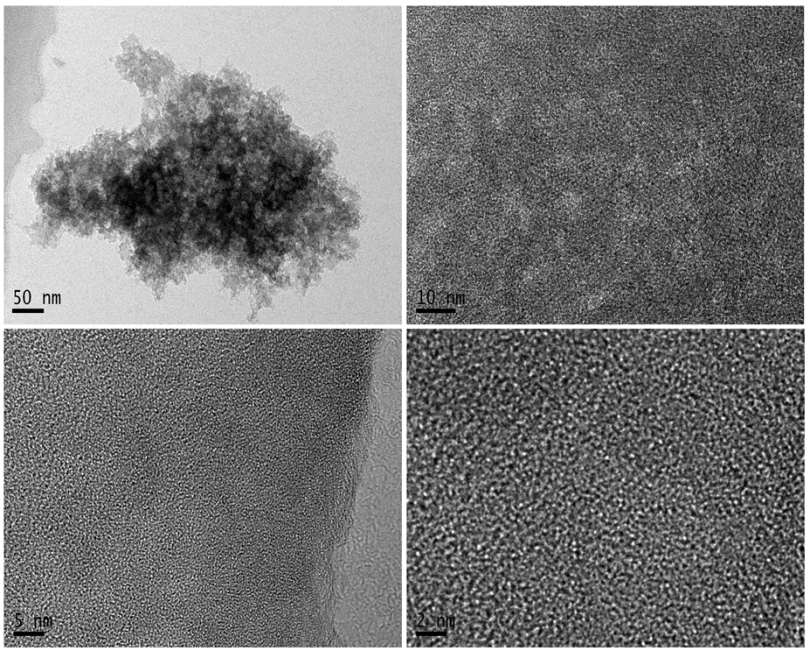

Fig. S14 TEM images for NOP-6.

9. BET linear plot for NOP-1~6 (Fig. S15)

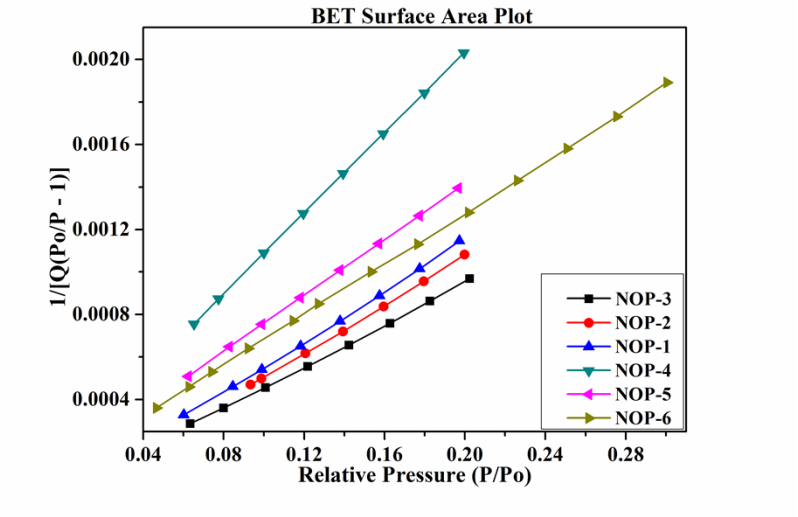

Fig. S15 BET linear plot for NOP-1~6

10. T-plot analysis for NOP-3 and NOP-6(Fig. S16 and Fig. S17)

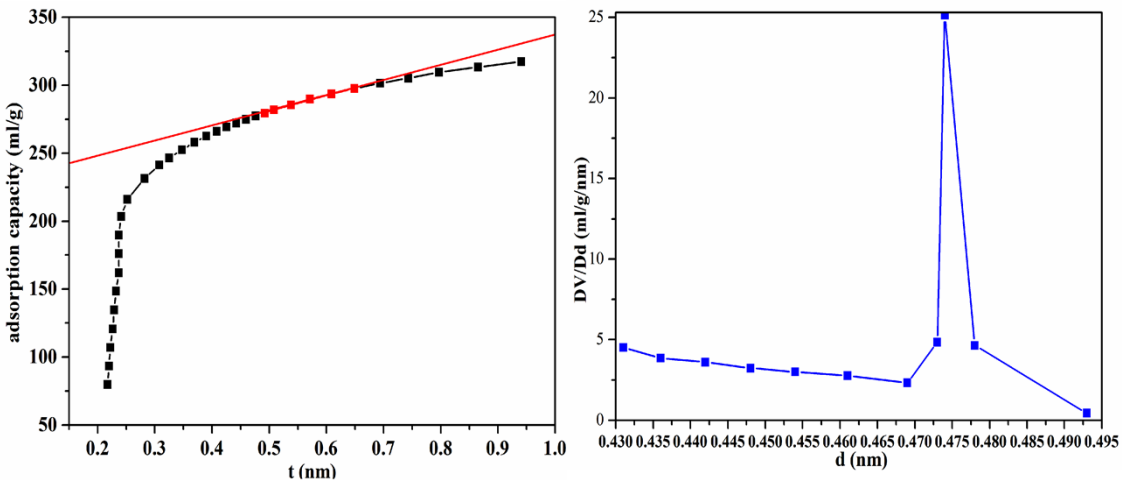

Fig. S16 T-plot analysis for NOP-3.

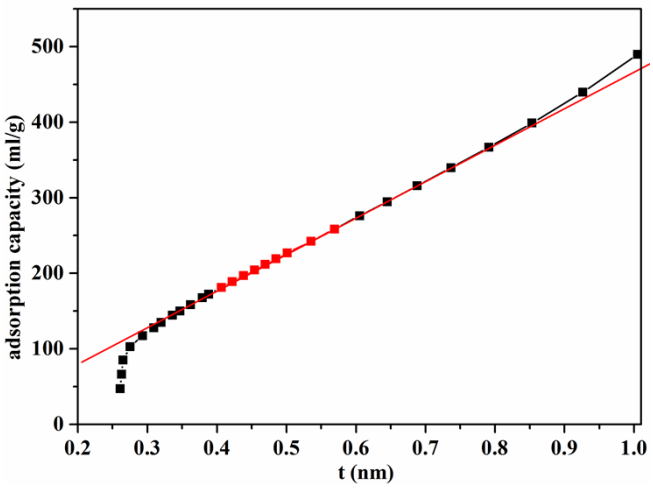

Fig. S17 T-plot analysis for NOP-6.

10. TGA and DTG curves of NOP-3 and NOP-6(Fig. S18)

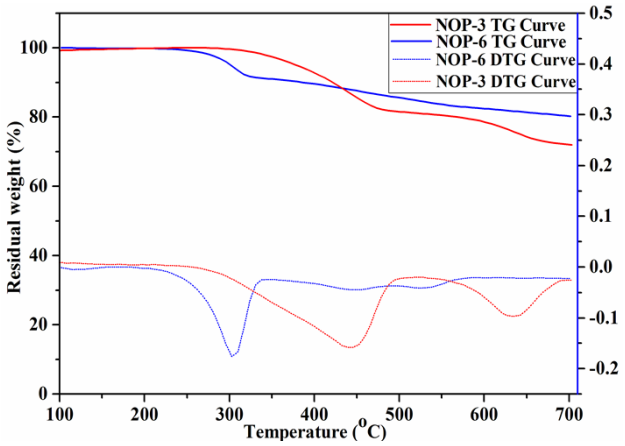

Fig. S18 TGA and DTG curves of NOP-3 and NOP-6 in Ar flow.

11. TGA curves for NOP-1 ~ NOP-5(Fig. S19)

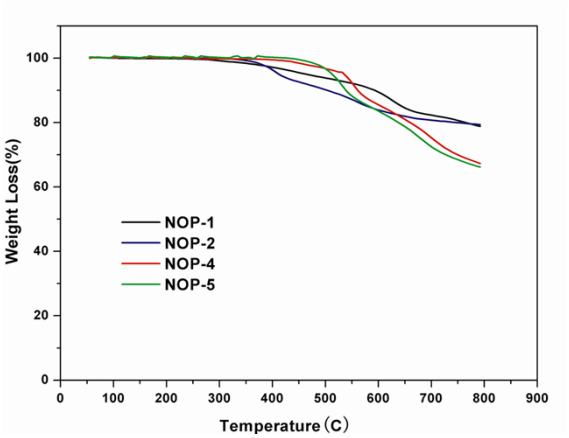

Fig. S19 TGA curves for NOP-1, NOP-2, NOP-4 and NOP-5 in Ar flow.

12. The CO2 uptake of NOP-1, NOP-2, NOP-4 and NOP-5

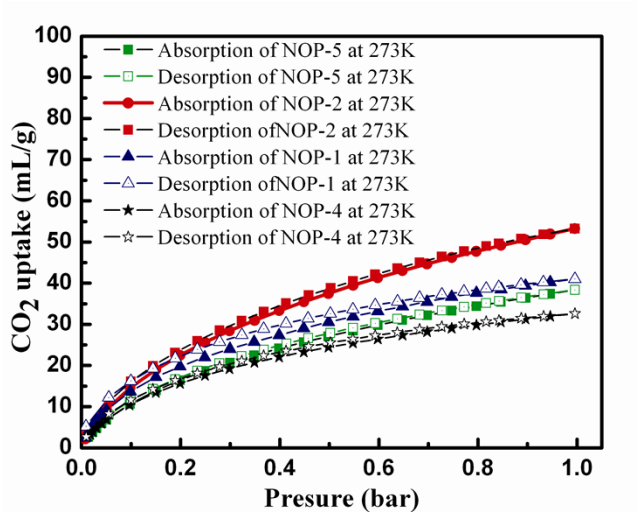

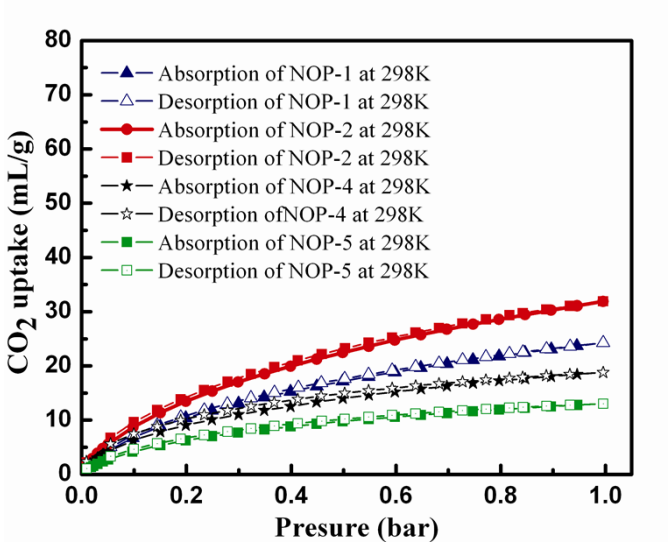

Fig.S20 Carbon dioxide adsorption and desorption isotherms at 273 K and 298K

13. Calculation of the isosteric enthalpies (Qst)

To calculate the isosteric enthalpies (Qst) of polymer NOP-3 and NOP-6 toward CO_2, the adsorption isotherms were measured at temperatures 273K and 298K. The collected data for each sample was fitted to Clausius−Clapeyron equation:

$$\ln P = \frac{Q_{st}}{RT} + C$$

where P, T, R, and C are the pressure, temperature at the equilibrium state, the gas

constant, and equation constant, respectively.

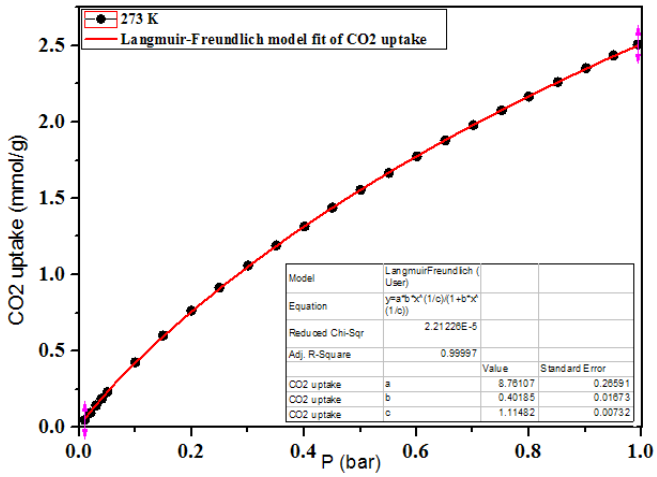

Fig. S21 Clausius−Clapeyron equation fit line for NOP-3 at 273K

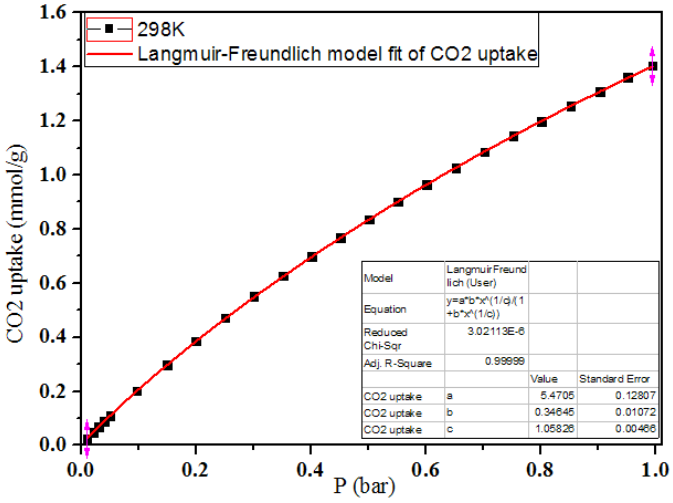

Fig. S22 Clausius−Clapeyron equation fit line for NOP-3 at 298K

Pressure as a function of the amount of CO2 adsorbed was determined by the Langmuir-Freundlich model for the isotherms.

y=a*b*xˆ(1/c)/(1+b*xˆ(1/c))

where y = moles adsorbed at saturation, x = pressure; a, b and c = constants; which can be used to calculate the pressure P.

14. The cycle experiments of CO2 uptake of NOP-3

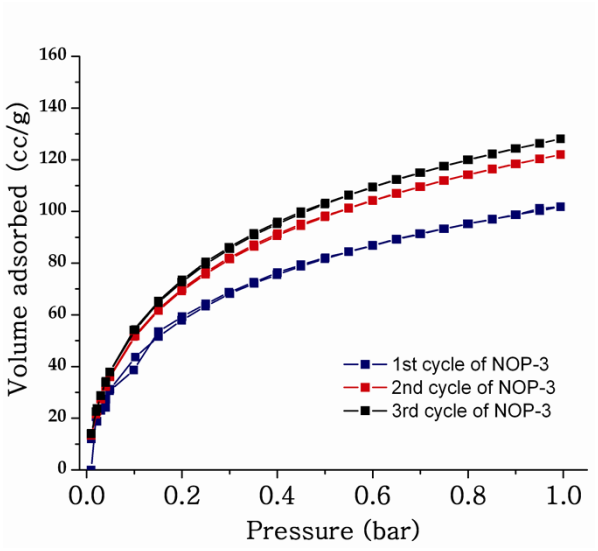

Fig.S23 the cycle experiments of CO_2 uptake of NOP-3 at 273K(Before each measurement, the sample was degassed for 8 h at 180 °C under vacuum.)

15. Ideal method for CO_2 over N_2 selectivity for NOP-3 and NOP-6

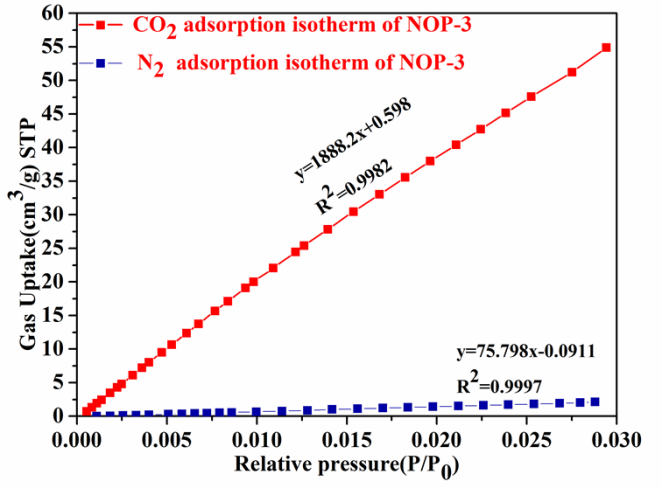

Fig.S24 Ideal method for CO_2 over N_2 selectivity for NOP-3

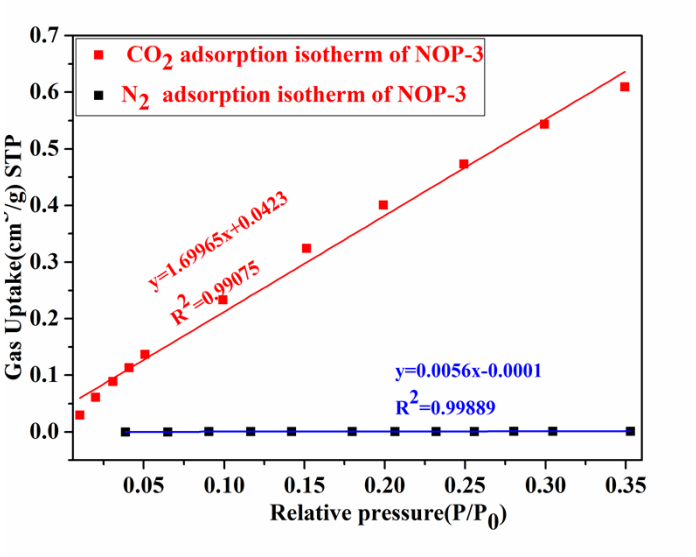

Fig.S25 Ideal method for CO_2 over N_2 selectivity for NOP-6

16. IAST method for CO_2 over N_2 selectivity for NOP-3 and NOP-6

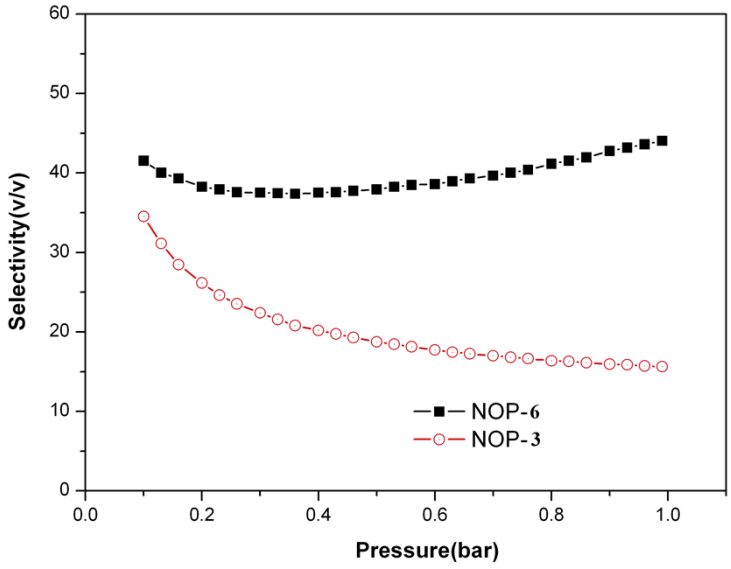

Fig.S26 IAST method for CO_2 over N_2 selectivity for NOP-3 and NOP-6

17. The photograph of the sample NOP-3 and NOP-6

Fig.S27 The photograph of the sample NOP-3

Fig.S28 The photograph of the sample NOP-6